

Article

Use of Zirconium Phosphate-Sulphate as Acid Catalyst for Synthesis of Glycerol-Based Fuel Additives

Maria Luisa Testa ¹, Valeria La Parola ¹, Farah Mesrar ², Fatiha Ouanji ², Mohamed Kacimi ^{2,*}, Mahfoud Ziyad ^{2,3} and Leonarda Francesca Liotta ^{1,*}

¹ Istituto per lo Studio dei Materiali Nanostrutturati (ISMN)-CNR, via Ugo La Malfa, 153, 90146 Palermo, Italy; marialuisa.testa@cnr.it (M.L.T.); valeria.laparola@cnr.it (V.L.P.)

² Université Mohammed V, Faculté des Sciences, Département de Chimie, Laboratoire de Physico-chimie des Matériaux et Catalyse, B.P. 1014 Rabat, Morocco; mesrar.farah@hotmail.com (F.M.); fatiha.ouanji@gmail.com (F.O.); mahfoudziyad@gmail.com (M.Z.)

³ Hassan II Academy of Science and Technology, 10000 Rabat, Morocco

* Correspondence: m_kacimi2000@yahoo.fr (M.K.); leonardafrancesca.liotta@cnr.it (L.F.L.); Tel.: +39-091-6809371 (L.F.L.)

Received: 17 January 2019; Accepted: 24 January 2019; Published: 2 February 2019



Abstract: In the present work, zirconium phosphates and mixed zirconium phosphate–sulphate acid catalysts have been investigated in the acetylation of glycerol in order to obtain acetins as fuel additives. The following catalysts with chemical composition, $Zr_3(PO_4)_4$, $Zr(SO_4)_2$, $Zr_2(PO_4)_2SO_4$, $Zr_3(PO_4)_2(SO_4)_3$ and $Zr_4(PO_4)_2(SO_4)_5$ have been prepared and characterized by acid capacity measurements, BET, XRD, FT-IR, XPS. The surface chemical composition in terms of P/Zr and S/Zr atomic ratios was monitored in the fresh and used catalysts. $Zr_3(PO_4)_2(SO_4)_3$ and $Zr_4(PO_4)_2(SO_4)_5$ showed the highest acidity associated with the synergic effect of two main crystalline phases, $Zr_2(PO_4)_2SO_4$ and $Zr(SO_4)_2 \cdot 4H_2O$. The reactions of glycerol acetylation were carried out by using a mass ratio of catalyst/glycerol equal to 5 wt% and molar ratio acetic acid/glycerol equal to 3:1. The glycerol conversion versus time was investigated over all the prepared samples in order to identify the best performing catalysts. Over $Zr_3(PO_4)_2(SO_4)_3$ and $Zr_4(PO_4)_2(SO_4)_5$ full glycerol conversion was achieved in 1 h only. Slightly lower conversion values were registered for $Zr_3(PO_4)_4$ and $Zr_2(PO_4)_2SO_4$, while $Zr(SO_4)_2$ was the worst catalyst. $Zr_4(PO_4)_2(SO_4)_5$ was the most selective catalyst and was used for recycling experiments up to five cycles. Despite a modest loss of activity, a drastic decrease of selectivity to tri- and diacetin was observed already after the first cycle. This finding was attributed to the leaching of sulphate groups as detected by XPS analysis of the spent catalyst.

Keywords: acetylation; glycerol; acetins; acid catalysts; zirconium phosphate–sulphate

1. Introduction

Nowadays due to rapidly rising oil prices and the negative environmental impacts of fossil fuels, the world faces energy and environmental crises. Various harmful gases are emitted during the combustion of fossil fuels, causing severe problems for the environment and human health. The use of clean and sustainable renewable energies is one of the most envisaged solutions for the future of energy and biodiesel presents itself as an alternative sustainable fuel. Biodiesel, a mixture of fatty acid methyl ester (FAME), is generally produced by the transesterification of methanol of triglycerides contained in vegetable oils. One of the main drawbacks of the biodiesel production process is the formation of glycerol (~10% wt) as the principal byproduct. During the last few decades, glycerol production increased, causing the price of glycerol to decrease and consequently creating several

problems for biodiesel production industries. Nowadays glycerol is used as an additive in food, tobacco and pharmaceuticals but its use as feedstock for the production of added-value compounds such as bioplastic, platform chemicals and biofuel additives is quite attractive. Due to its structure as a polyol with both primary and secondary -OH, glycerol represents a versatile molecule which can be subjected to plenty of reactions for the production of several high-value chemicals [1].

Many efforts are being made to turn the processes into “green” chemical reactions by working on heterogeneous catalysts that can be used several times and are both easier and safer to handle. Moreover, the development of the heterogeneous catalysts reduces costs for large commercial application.

The catalytic oxidation of glycerol can be carried out by mono or bimetallic supported catalysts, such as Pd, Pt and Au on carbon, in order to obtain dihydroxyacetone, [2] glyceric acid [3] or lactic acid [4]. Through the steam reforming process of glycerol it is possible to produce H₂ by using Pt/Al₂O₃ [5]. Several studies on glycerol reduction to 1, 2-propanediol or 1, 3-propanediol, to acrolein, to lactic acid were carried out by the use of Zn, Cu, Pd, Pt, and Co catalysts [6,7].

Among the different reactions, the esterification of glycerol (Figure 1) into acetins is one of the most interesting reactions. Due to the versatile industrial application of the final products, it can be applied to anything from cosmetic to fuel additives [8].

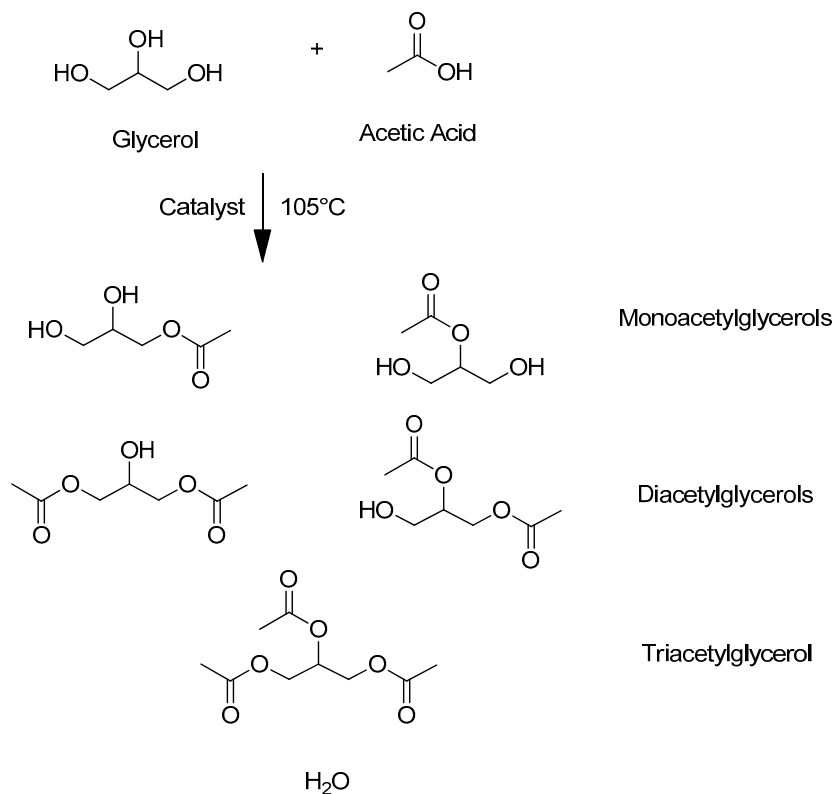


Figure 1. Esterification of glycerol with acetic acid.

In fact, triacetin is used as an antiknock additive for gasoline, where it also improves the cold and viscous properties of biodiesel. Diacetin is a good solvent for various dyes and presents good properties as a plasticizer. Finally, monoacetin is a good raw material for the production of biodegradable polyesters. It is also used as food additive and in the manufacture of dynamite due to its explosive properties [9].

Some of us have reported recently that sulfonic and phosphonic acid functionalized mesoporous silicas show high activity and good stability for glycerol acetylation to triacetin [10,11]. Different types of heterogeneous acid catalysts were studied (Amberlyst-15, zeolite, organic-inorganic sulphonic or

phosphonic silica). In both studies, it was found that the catalytic activity of the materials was related not only to their acid capacities but also to the strength and the surface density of the acidic sites.

In the last decade, the use of some functionalized zirconia acid catalysts for the glycerol acetylation was reported. $\text{HClSO}_3/\text{ZrO}_2$ and $\text{H}_2\text{SO}_4/\text{ZrO}_2$ were found to be very active for both the conversion and the selectivity [12]. Reddy et al. [13] concluded that the acetylation reaction could be catalyzed not only by the Brønsted acid site but also by Lewis acid sites. Moreover, Silva et al. [14] reported that by using zirconia catalysts, some drawbacks such as high pressure reaction, acid site deactivation and high molar ratio acetic acid/glycerol occurred. In order to increase the performance of the catalysts, a substitution of phosphate by sulphate with an increment of the acidity of the catalysts could be eligible. Ce and Th phosphates and ZrNbPO_4 activated by Pt nanoparticles have been successfully used as solid acid catalysts for the conversion of several biomass-based components to chemicals [15,16]. To our knowledge, only a few reports concerning mixed Zr phospho-sulphates have been reported in the literature [17–19] and no application to glycerol acetylation has been performed so far.

Among the recent literature, it is worth mentioning a short review highlighting the application of zirconium phosphate and its derivatives in the field of heterogeneous catalysis, especially in acid-catalyzed reactions such as dehydration, isomerization, and ester hydrolysis reactions [20]. By tuning the surface area and acidic properties, the material porosity and the functional groups anchored at the surface, it is possible to design and synthesize tailored catalysts with optimized properties for specific catalytic process.

As a continuation of our interest towards the application of solid acid catalyst into glycerol acetylation for the production of added-value compounds, in the present work we focused our attention on the performances of sulphate and/or phosphate zirconia-derived catalysts. The relation between the material structure and the activity was studied, and, in particular, the co-presence of both acid anions was analyzed in terms of influence on the glycerol conversion and acetins selectivity. Moreover, in order to improve the experimental condition and reduce the drawbacks reported by Silva [14], glycerol acetylation reactions were carried out by using molar ratio acetic acid/glycerol corresponding to 3:1 and a mass ratio of catalyst/glycerol equal to 5 wt%, according to our previous studies [10,11]. Recycling experiments up to five cycles were performed on the most active and selective catalyst, $\text{Zr}_4(\text{PO}_4)_2(\text{SO}_4)_5$. The synthesized materials were analyzed by means of N_2 adsorption/desorption isotherms, X-ray diffraction (XRD), Fourier Transform infrared spectroscopy (FT-IR), X-ray photoelectron spectroscopy (XPS) and acid capacity measurements.

2. Results and Discussion

2.1. Characterization

The acid capacity was determined by titration with 0.01 M NaOH (aq), in terms of $\text{mmol H}^+ \text{g}^{-1}$ and is reported in Table 1. The values indicate that the co-presence of both sulphate and phosphate groups improve the acidity of the prepared materials.

Table 1. Textural properties in terms of specific surface area (BET) and total pore volume and acid capacity by NaOH titration determined for the zirconium phosphate–sulphate catalysts.

Sample	BET (m^2/g)	Vp (cm^3/g)	Acid Capacity ($\text{mmol H}^+/\text{g}$)
$\text{Zr}(\text{SO}_4)_2$	14.5	0.1	2.9
$\text{Zr}_4(\text{PO}_4)_2(\text{SO}_4)_5$	15.0	0.1	7.5 (2.76) ¹
$\text{Zr}_3(\text{PO}_4)_2(\text{SO}_4)_3$	12.5	0.1	5.0
$\text{Zr}_2(\text{PO}_4)_2\text{SO}_4$	11.0	0.09	3.2
$\text{Zr}_3(\text{PO}_4)_4$	105.0	0.3	2.0

¹ The acidity registered after 5 cycles.

Sulphate and mixed sulphate/phosphate samples have a small surface area, which is typical of crystalline materials. The surface area of these catalysts ranges between 10 and 15 m²g⁻¹ and the pore volume is 0.1 cm³g⁻¹. Zr₃(PO₄)₄ surface area is higher (105 m²g⁻¹), which points to an amorphous structure.

Figure 2 displays the N₂ adsorption/desorption isotherms for Zr₄(PO₄)₂(SO₄)₅ and for Zr₃(PO₄)₄ taken as representative samples.

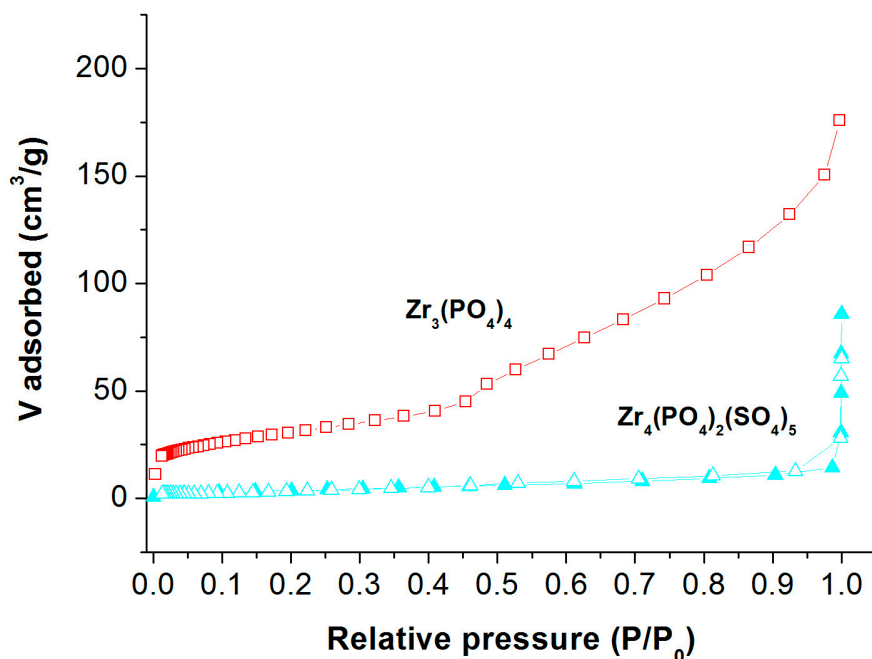


Figure 2. N₂ adsorption-desorption isotherms for two selected samples, Zr₃(PO₄)₄ and Zr₄(PO₄)₂(SO₄)₅.

Figure 3a shows the XRD patterns of the catalysts. The crystallinity of the samples decreased from the crystalline Zr(SO₄)₄, which exhibits a typical α orthorhombic phase [21], to the amorphous Zr₃(PO₄)₄ [22]. The mixed sulphate-phosphate salts show a decrease of crystallinity with fewer sulphate anions in the composition. All mixed samples are characterized by features typical of an orthorhombic Zr₂(PO₄)₂SO₄ phase (ICSD #202395). Moreover, other diffraction peaks (at ~13.8°, 18.15°, 20.55°, 25.6°, 30.05, 38.75° 2 θ) attributed to segregated tetrahydrate zirconium sulphate phase, Zr(SO₄)₂·4H₂O (ICSD #75474) were detected in both Zr₃(PO₄)₂(SO₄)₃ and Zr₄(PO₄)₂(SO₄)₅ [23]. Furthermore, a perusal of the pattern of Zr(SO₄)₄ revealed the presence of the Zr(SO₄)₂·4H₂O phase (ICSD #75474) also in such sample.

In Figure 3b an enlargement of the spectra of Zr(SO₄)₂ and Zr₄(PO₄)₂(SO₄)₅ is shown along with the reference patterns. No reflections, due to crystalline ZrO₂, are present.

In the FT-IR spectra (Figure 4), bands in the region ~3400–3200 cm⁻¹ corresponding to the stretching vibration of -OH groups were detected. The broadness of the bands indicates the presence of intermolecular H bonds in the samples. At 1640 cm⁻¹ the H₂O deformation mode appeared. At 1400 and 1250 cm⁻¹ the S=O stretching bands of sulphate species are visible, while the phosphate group, (PO₄)³⁻, is characterized by the intense band at around 1050 cm⁻¹ [24–26]. In the same region the stretching of surface monosulphates (S-O) is known to occur. In the range 700–500 cm⁻¹, vibrations of O-S-O and O-P-O groups take place. Overall, no significant differences in the wavenumber position were observed, suggesting that the contribution of the sulphate and phosphate species is additive without any mutual interaction.

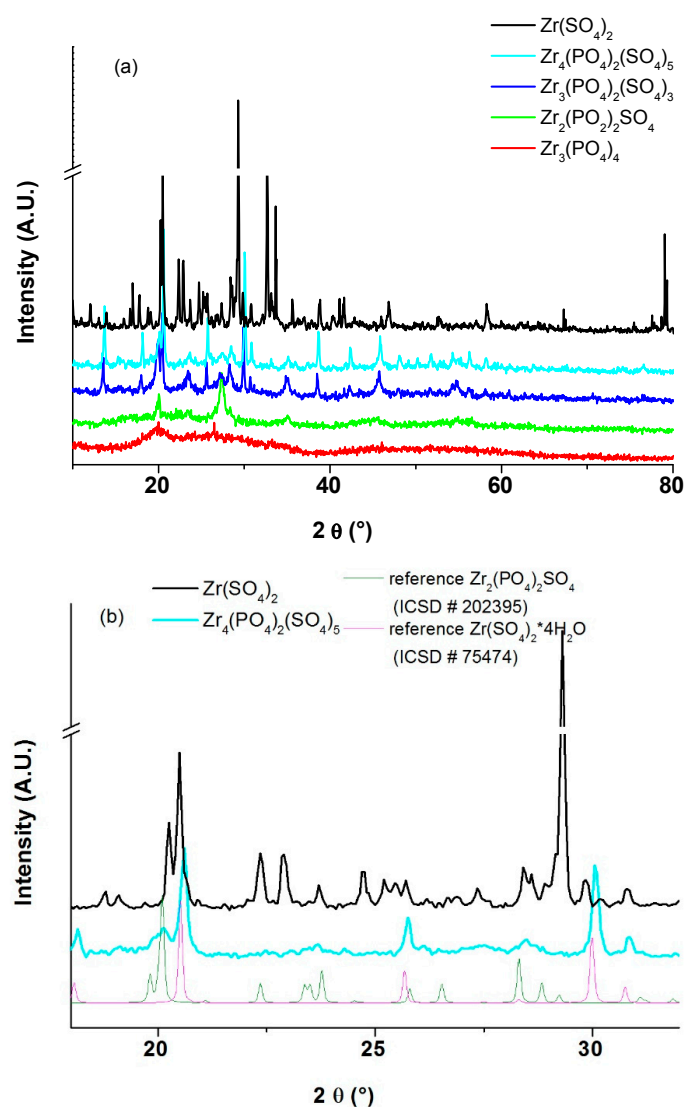


Figure 3. (a) XRD patterns of the Zirconium Phosphate-Sulphate catalysts. (b) XRD enlarged patterns of $\text{Zr}(\text{SO}_4)_2$ and $\text{Zr}_4(\text{PO}_4)_2(\text{SO}_4)_5$ along with the reference files, $\text{Zr}_2(\text{PO}_4)_2\text{SO}_4$ (ICSD #202395) and $\text{Zr}(\text{SO}_4)_2 \cdot 4\text{H}_2\text{O}$ (ICSD #75474).

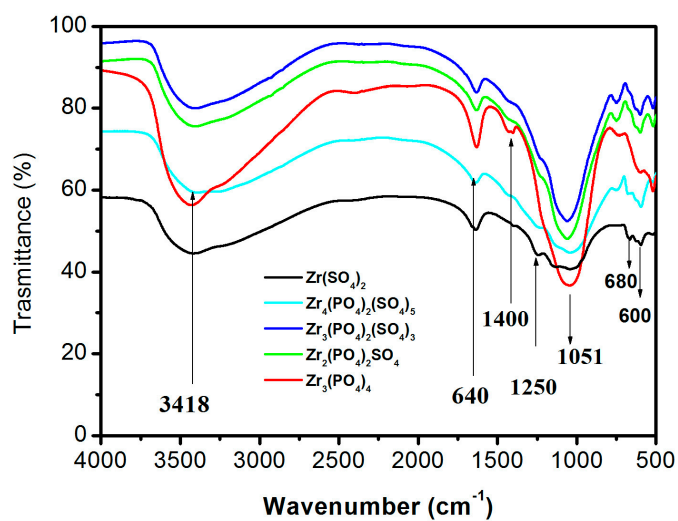


Figure 4. FT-IR spectra of the zirconium phosphate-sulphate catalysts.

In order to evaluate the surface composition of the samples, XPS analysis was performed. The Zr 3d region (Figure 5), showing the 3d5/2 and 3d3/2 components, was fitted constraining the distance between the two components at 2.4 eV. Each component showed two peaks. For the Zr3d5/2 component the two peaks are centred at 182 and 184 eV. The low energy peak is attributed to ZrO₂, while the 184 eV peak is due to Zr(IV) bound to an electroactive species such as sulphur or phosphorous [23,27]. The high BE peak value registered for Zr₃(PO₄)₂(SO₄)₃ and Zr₄(PO₄)₂(SO₄)₅ is at 185.2 eV, indicative of a shift of the electron density from the Zr site towards the Sulphate /Phosphate groups and an enhancement of the Lewis acidity of Zr centre. As shown in Table 2 and Figure 5, samples Zr₃(PO₄)₂(SO₄)₃ and Zr₄(PO₄)₂(SO₄)₅ do not show the component due to ZrO₂. By looking at the Zr3d5/2 spectra of Zr₄(PO₄)₂(SO₄)₅ after catalytic cycles I and V (See Figure 6) an insurgence of a doublet at low energy which increases with the catalytic cycles is observed. The Zr 3d5/2 position of this doublet is at 183.0 ± 0.2 eV, which can be attributed to the formation of Zr(OH)₄ [28]. Moreover, the high BE peak shifted to 184 eV, indicating a modification of the electron density distribution between the Zr and sulphate-phosphate groups. S2p and P2p are centred for all samples at 170.5 and 135.2 eV respectively. These values are typical of sulphate/phosphate species and are in agreement with previous reports on sulphated and phosphated zirconia powder. If we look at the XPS derived atomic ratio (see Table 2) we observe that all samples show a surface composition analogous to the bulk composition. After the use of Zr₄(PO₄)₂(SO₄)₅ in the glycerol acetylation, we observed that the position of S2p and P2p peaks do not change after catalytic cycles, but a leaching of the sulphate group occurs. This fact accounts for the decrease of the acidity and hence for the activity registered after the fifth catalytic cycle.

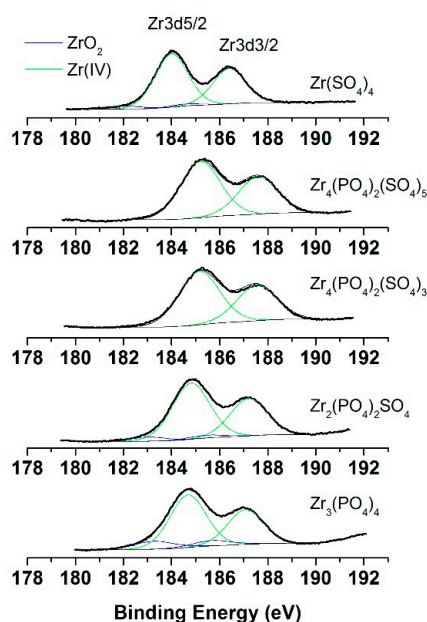


Figure 5. Zr3d XPS region for pure and mixed catalysts.

Table 2. Zr3d5/2 binding energy and theoretical and XPS derived atomic concentration.

Sample	Zr3d5/2 (eV)	Zr/P/S/O (at.%) Theoretical	Zr/P/S/O (at.%) XPS Derived
Zr(SO ₄) ₂	182.1 (5%)–184.0 (95%)	9/0/18/73	7/0/21/70
Zr ₄ (PO ₄) ₂ (SO ₄) ₅	185.2 (100%)	10/5/13/72	10/4/17/69
First cycle	182.8 (8%)–184.0 (92%)		13/5/11/71
Fifth cycle	183.2 (9%)–184.0 (91%)		13/7/7/73
Zr ₃ (PO ₄) ₂ (SO ₄) ₃	185.2 (100%)	11/7/11/71	10/5/17/68
Zr ₂ (PO ₄) ₂ SO ₄	183.0 (7%)–184.7 (93%)	12/12/6/71	11/14/8/66
Zr ₃ (PO ₄) ₄	183.3 (14%)–184.7 (86%)	13/17/0/70	14/22/0/64

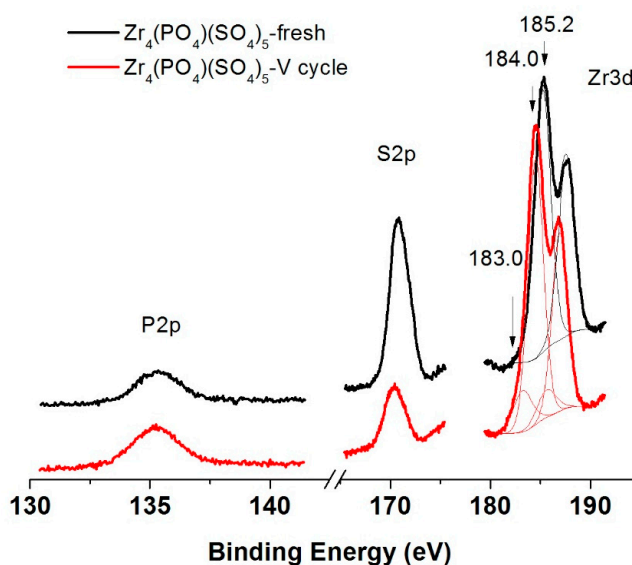


Figure 6. P2p, S2p and Zr3d XPS region of $Zr_4(PO_4)_2(SO_4)_5$ fresh and after five catalytic cycles.

2.2. Catalytic Activity

The acetylation reaction was studied in the presence of different solid acids, and the catalytic activity of the catalysts was evaluated in terms of the conversion of glycerol and selectivity toward monoacetylglycerol, diacetylglycerol and triacetylglycerol. The reaction was carried out at a temperature of 105 °C with an acetic acid: glycerol molar ratio corresponding to 3:1. The glycerol conversion versus time (3 h) over various catalysts is displayed in Figure 7. $Zr_3(PO_4)_2(SO_4)_3$, $Zr_4(PO_4)_2(SO_4)_5$ results performed highly in acetylation, giving full glycerol conversion in 1 h only, while the other samples showed lower activity. Almost 100% glycerol conversion was registered for $Zr_3(PO_4)_4$ and $Zr_2(PO_4)_2SO_4$ after 3 h. Conversely, $Zr(SO_4)_2$ was the worst performing catalyst, reaching only ~60% of glycerol conversion during the reaction time investigated.

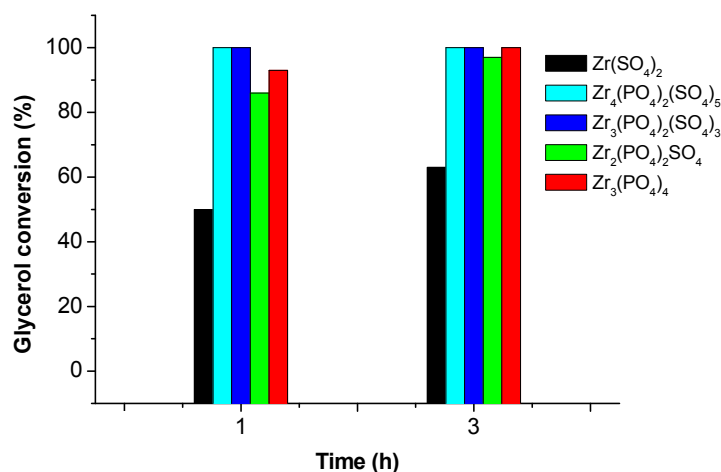


Figure 7. Conversion of glycerol over different Zr Phosphate-Sulphate catalysts.

Based on the promising results in glycerol conversion registered after only 1 h of reaction over $Zr_3(PO_4)_2(SO_4)_3$, $Zr_4(PO_4)_2(SO_4)_5$, the selectivity to acetins versus time was studied for such samples. Figure 8a,b display the selectivity to the three acetins as a function of time for the most active catalysts, $Zr_3(PO_4)_2(SO_4)_3$ and $Zr_4(PO_4)_2(SO_4)_5$ respectively. The glycerol conversion was completed after 1 h of reaction for both catalysts, and remained constant to 100% during the test. After 5 h of reaction

$Zr_3(PO_4)_2(SO_4)_3$ showed a distribution of acetins: mono acetins at 15%, diacetins at 50%, and triacetins at 35%, while the $Zr_4(PO_4)_2(SO_4)_5$ showed 15%, diacetins 48%, and triacetins 39%. This latter catalyst, which exhibited the best product distribution, was left reacting up to 24 h in order to evaluate if further increase in triacetin can be obtained. Indeed, after 24 h reaction, the obtained amount of di- and triacetin was 46% and 43%, respectively.

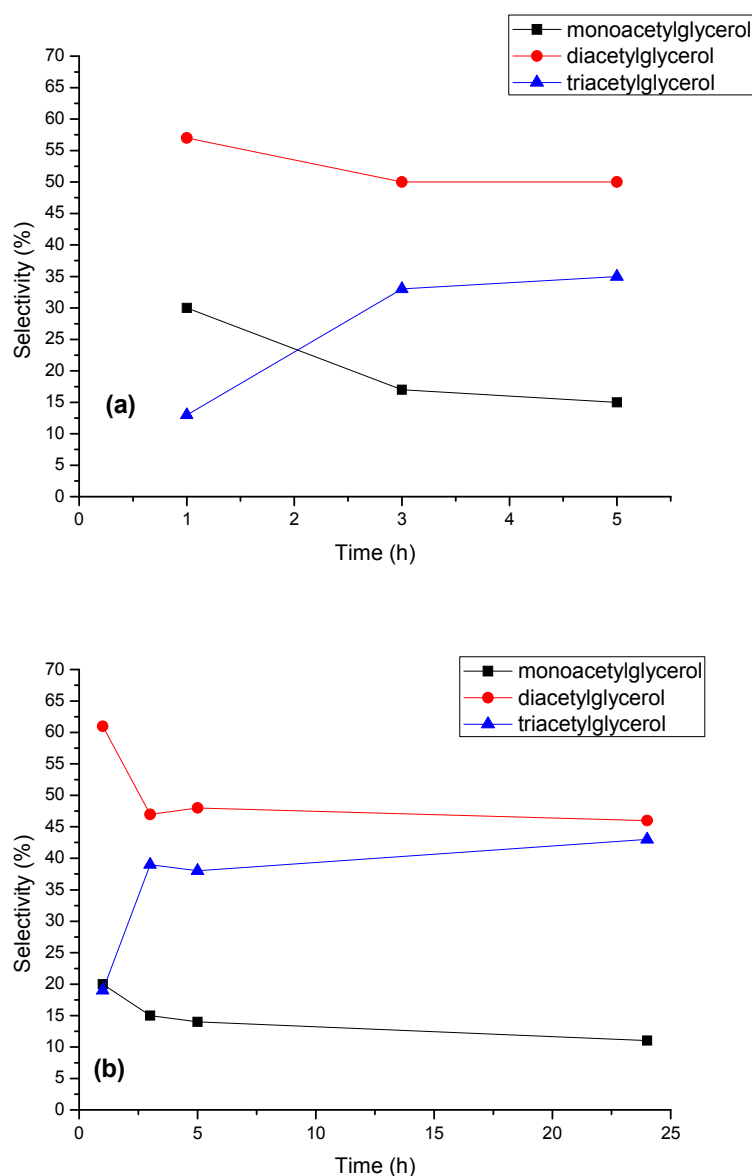


Figure 8. Selectivity of acetylated products over (a) $Zr_3(PO_4)_2(SO_4)_3$ and (b) $Zr_4(PO_4)_2(SO_4)_5$. Glycerol conversion was complete (100%).

Based on the so far reported promising results, the stability of the material was investigated. Recycle runs of glycerol acetylation over $Zr_4(PO_4)_2(SO_4)_5$ during 1 h, were carried out. As shown in Figure 9a, a slight decrease of glycerol conversion (96%) is evident from the second cycle. An important decrease occurred during the fourth cycle when the glycerol conversion was only 80%. In the last cycle, the percentage settled to 77%. Concerning the selectivity (Figure 9b), as expected, during the cycles the mono- and diacetylglycerol became the principal final product with 79% and 21% respectively obtained during the last recycle run. The same selectivity trend was already observed during our previous studies [10,11].

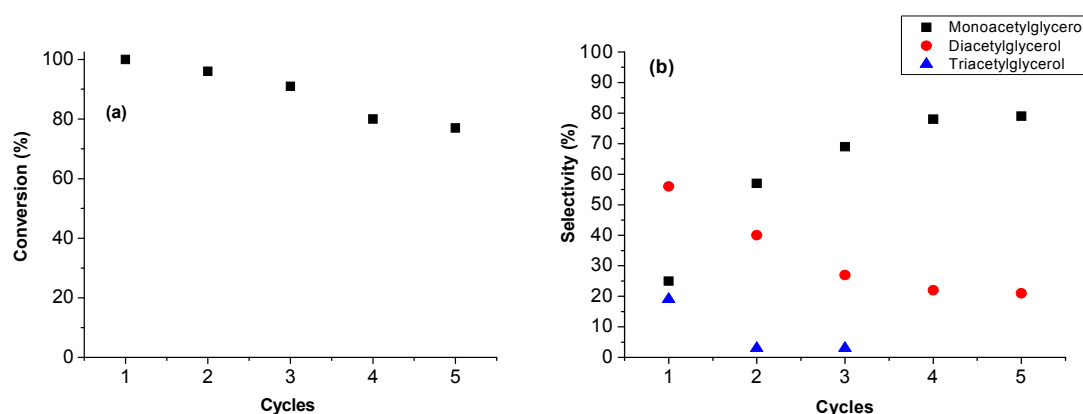


Figure 9. Recycling runs during 1 h of the glycerol acetylation over $Zr_4(PO_4)_2(SO_4)_5$. Both glycerol conversion (a) and selectivity (b) towards the acetins are shown.

As mentioned in the characterization paragraph, the spent $Zr_4(PO_4)_2(SO_4)_5$ catalyst was analysed after the first and the fifth catalytic cycle with XPS and acidic titration. As shown in Table 1, an important decrease of the acidity of the material from 7.5 to 2.76 mmol H^+ / g is evident. It can be postulated that in the reaction medium the hydrolysis of the $Zr(SO_4)_4 \cdot 4H_2O$ phase to H_2SO_4 and $Zr(OH)_4$ takes place, with a consequent leaching of sulphate groups. A similar hydrolysis process can be assumed for mixed Zr Phosphate-Sulphate catalysts. This hypothesis was confirmed by XPS analysis of the recovered $Zr_4(PO_4)_2(SO_4)_5$ catalyst, which showed an important decrease of the sulphate groups on the surface and a concomitant appearance of a doublet that can be attributed to $Zr(OH)_4$. Moreover, the binding energy of $Zr3d_{5/2}$, attributed to Zr(IV) interacting with sulphate-phosphate groups, shifted from 185 to 184 eV ca. as found for the other three catalysts. Such modification pointing to a decrease of Lewis acidity of Zr site accounts for the decrease of catalytic activity and selectivity to triacetins during reaction.

The high activity of $Zr_3(PO_4)_2(SO_4)_3$ and $Zr_4(PO_4)_2(SO_4)_5$ samples was related to the presence of two main crystalline phases, $Zr_2(PO_4)_2SO_4$ and $Zr(SO_4)_2 \cdot 4H_2O$ which seem synergistically to contribute to the higher acidity of these materials. According to XPS, the zirconium atom showed a binding energy higher than that found for Zr(IV) in the other three catalysts. This difference is indicative of a shift of electron density from the Zr towards the sulphate/phosphate groups, which accounts for the higher Lewis acidity [25]. Based on this finding, it can be inferred that the glycerol acetylation reaction involves the coordination of the carboxylic group of the acetic acid on the Lewis zirconium site. Such coordination promotes the nucleophilic attack of the alcoholic group of glycerol on the activated carbonyl of acetic acid.

3. Materials and Methods

3.1. Catalysts Preparation

All the used catalysts were synthesized by precipitation. Zirconium phosphate and zirconium sulphate catalysts were prepared by adding $ZrOCl_2 \cdot 8H_2O$ (CAS 13520-92-8) to H_3PO_4 (CAS 766-38-2) or H_2SO_4 (CAS 7664-93-9) acid solutions. Mixed zirconium phosphates-sulphates were obtained by dissolving $ZrOCl_2 \cdot 8H_2O$ into stoichiometric mixtures of H_3PO_4 and H_2SO_4 acid solutions in order to obtain catalysts with the following composition: $Zr_3(PO_4)_4$, $Zr(SO_4)_2$, $Zr_2(PO_4)_2SO_4$, $Zr_3(PO_4)_2(SO_4)_3$ and $Zr_4(PO_4)_2(SO_4)_5$. The obtained gels were stirred for 2 h at 80 °C until dry, then further dried in an oven at 110 °C overnight. Since phosphate and sulphate species can rapidly degrade under humidified air, the prepared catalysts were stored in a desiccator.

3.2. Characterization Methods

Acid capacity and concentration of sulfonic groups was determined by titration with 0.01 M NaOH (aq) [29]. In a typical experiment, 0.1 g of solid was added to 10 mL of deionized water. The resulting suspension was allowed to equilibrate and thereafter was titrated by the dropwise addition of 0.01 M NaOH solution using phenolphthalein as a pH indicator.

The textural characterization was performed with a Carlo Erba Sorptomat 1900 instrument (Fisons, UK). The fully computerized analysis of the nitrogen adsorption isotherm at 77 K allowed us to estimate the specific surface areas of the samples through the BET method in the standard pressure range 0.05–0.3 p/p₀. By analysis of the desorption curve, using the BJH calculation method, the pore size distribution was also obtained. The total pore volume (V_p) was evaluated on the basis of the amount of nitrogen adsorbed at a relative pressure of about 0.98.

X-ray diffraction (XRD) analyses was performed using X-ray diffraction (XRD) measurements on a Bruker-Siemens D5000 X-ray powder diffractometer (Bruker AXS, Karlsruhe, Germany) equipped with a Kristalloflex 760 X-ray generator and a curved graphite monochromator using Cu K α radiation (40 kV/30 mA). A proportional counter and 0.05° step sizes in 2 θ were used. The assignment of the crystalline phases was based on the ICSD powder diffraction file cards.

Fourier transform infrared (FT-IR) spectra were recorded at room temperature between 400 and 4000 cm⁻¹ with a Bruker Equinox spectrometer (Wissembourg, France) using self-supporting KBr disks. Before recording FT-IR spectra the samples were pretreated in an oven overnight at 100 °C.

The X-ray photoelectron spectroscopy (XPS) analyses of the powders were performed with a VG Microtech ESCA 3000 Multilab (VG Scientific, Sussex, UK), using Al K α source (1486.6 eV) run at 14 kV and 15 mA, and CAE analyser mode. For the individual peak energy regions, a pass energy of 20 eV set across the hemispheres was used. The constant charging of the samples was removed by referencing all the energies to the C 1 s peak energy set at 285.1 eV, arising from adventitious carbon. Analysis of the peaks was performed using the CASA XPS software. The binding energy values are quoted with a precision of ± 0.15 eV and the atomic percentage with a precision of $\pm 10\%$.

3.3. Esterification Reaction

In a typical experiment, acetic acid (32.6 mmol, Aldrich CAS 64-91-7) was added to a mixture of glycerol (1 g, 10.87 mmol, Aldrich CAS 56-81-5) and catalysts (50 mg). Mass ratio of catalyst/glycerol corresponding to 5%wt and molar ratio acetic acid:glycerol corresponding to 3:1 were used. The reaction was carried out in a 25 mL round bottom flask connected to a water-cooled condenser. The reaction mixture was continuously stirred using a magnetic stirrer and refluxed at 105 °C. The products were analysed by GC-MS on a GCMS-QP5050A Shimadzu mass spectrometer with ionisation energy of 70 eV and their chromatograms were in accord with those obtained from reference samples.

The recycling experiments were performed over the most active catalyst Zr₄(PO₄)₂(SO₄)₅. After the reaction the material was filtered, washed with methanol in order to clean the surface, dried, activated at 120 °C overnight and reused during five cycles.

4. Conclusions

Mixed Zr phosphate–sulphate catalysts with the formula Zr(SO₄)₂, Zr₄(PO₄)₂(SO₄)₅, Zr₃(PO₄)₂(SO₄)₃, Zr₂(PO₄)₂SO₄ and Zr₃(PO₄)₄ were prepared and characterized by several techniques such as acid capacity measurements, BET, XRD, FT-IR and XPS. Glycerol acetylation tests were performed over such acid catalysts. Zr₃(PO₄)₂(SO₄)₃ and Zr₄(PO₄)₂(SO₄)₅ showed the best catalytic performances in terms of glycerol acetylation and triacetin selectivity that were associated to the high Lewis acidic character of zirconium atom induced by the synergic presence of both sulphate-phosphate groups. Recycling tests performed over Zr₄(PO₄)₂(SO₄)₅ evidenced that despite a modest loss of activity, a drastic decrease of selectivity to tri- and diacetin occurs already after the first cycle, due to leaching of sulphate groups.

Author Contributions: This study was conducted through contributions of all authors. M.L.T. and V.L.P. equally contributed to the paper, performing experiments and characterizations and writing some parts of the paper. F.M. and F.O. prepared the catalysts. M.K. and M.Z. designed the nature of catalysts and planned the study. L.F.L. completed the writing of the manuscript in its final form.

Funding: This research received no external funding.

Acknowledgments: The authors are grateful to Hassan II Academy of Sciences and Technology for the financial support kindly provided to this research. The bilateral project CNR-CNRST (201–2015) is acknowledged.

Conflicts of Interest: The authors declare no conflict of interest.

References

1. Climent, M.J.; Corma, A.; De Frutos, P.; Iborra, S.; Noy, M.; Velty, A.; Concepción, P. Chemicals from biomass: Synthesis of glycerol carbonate by transesterification and carbonylation with urea with hydrotalcite catalysts. The role of acid–base pair. *J. Catal.* **2010**, *269*, 140–149. [[CrossRef](#)]
2. Hu, W.; Knight, D.; Lowry, B.; Varma, A. Selective oxidation of glycerol to dihydroxyacetone over Pt–Bi/C catalyst: Optimization of catalyst and reaction conditions. *Ind. Eng. Chem. Res.* **2010**, *49*, 10876–10882. [[CrossRef](#)]
3. Ang, G.T.; Tan, K.T.; Lee, K.T. Recent development and economic analysis of glycerol-free processes via supercritical fluid transesterification for biodiesel production. *Renew. Sustain. Energy Rev.* **2014**, *31*, 61–70. [[CrossRef](#)]
4. Lakshmanan, P.; Upare, P.; Le, N.T.; Hwang, Y.K.; Hwang, D.W.; Lee, U.H.; Chang, J.S. Facile synthesis of CeO₂-supported gold nanoparticle catalysts for selective oxidation of glycerol into lactic acid. *Appl. Catal. A* **2013**, *468*, 260–268. [[CrossRef](#)]
5. Liu, B.; Greeley, J. Decomposition pathways of glycerol via C–H, O–H, and C–C bond scission on Pt (111): A density functional theory study. *J. Phys. Chem. C* **2011**, *115*, 19702–19709. [[CrossRef](#)]
6. Nakagawa, Y.; Tomishige, K. Heterogeneous catalysis of the glycerol hydrogenolysis. *Catal. Sci. Technol.* **2011**, *1*, 179–190. [[CrossRef](#)]
7. Katryniok, B.; Paul, S.; Belliere-Baca, V.; Rey, P.; Dumeignil, F. A long-life catalyst for glycerol dehydration to acrolein. *Green Chem.* **2010**, *12*, 1922–1925. [[CrossRef](#)]
8. Rahmat, N.; Abdullah, A.; Mohamed, A. Recent progress on innovative and potential technologies for glycerol transformation into fuel additives: A critical review. *Renew. Sustain. Energy Rev.* **2010**, *14*, 987–1000. [[CrossRef](#)]
9. Bagheri, S.; Jukapli, N.; Dabdawb, W.; Mansouri, N. Biodiesel-Derived Raw Glycerol to Value-Added Products: Catalytic Conversion Approach. In *Handbook of Composites from Renewable Materials*; Thakur, V.K., Thakur, M.K., Kessler, M.R., Eds.; Wiley: Hoboken, NJ, USA, 2017; Volume 3, pp. 309–366.
10. Testa, M.L.; La Parola, V.; Liotta, L.F.; Venezia, A.M. Screening of different solid acid catalysts for glycerol acetylation. *J. Mol. Catal. A Chem.* **2013**, *367*, 69–76. [[CrossRef](#)]
11. Beejapur, H.A.; La Parola, V.; Liotta, L.F.; Testa, M.L. Glycerol Acetylation over organic-inorganic Sulfonic or Phosphonic Silica Catalysts. *Chem. Sel.* **2017**, *2*, 4934–4941. [[CrossRef](#)]
12. Gonçalves, V.L.; Pinto, B.P.; Silva, J.C.; Mota, C.J. Acetylation of glycerol catalyzed by different solid acids. *Catal. Today* **2008**, *133*, 673–677. [[CrossRef](#)]
13. Reddy, P.S.; Sudarsanam, P.; Raju, G.; Reddy, B.M. Selective acetylation of glycerol over CeO₂–M and SO₄²⁻/CeO₂–M (M = ZrO₂ and Al₂O₃) catalysts for synthesis of bioadditives. *J. Ind. Eng. Chem.* **2012**, *18*, 648–654. [[CrossRef](#)]
14. Silva, L.N.; Gonçalves, V.L.; Mota, C.J. Catalytic acetylation of glycerol with acetic anhydride. *Catal. Commun.* **2010**, *11*, 1036–1039. [[CrossRef](#)]
15. Parangi, T.F.; Wani, B.N.; Chudasama, U.V. Acetalization of Carbonyl Compounds with Pentaerythritol Catalyzed by Metal(IV) Phosphates a solid Acid Catalysts. *Ind. Eng. Chem. Res.* **2013**, *52*, 8969–8977. [[CrossRef](#)]
16. Chen, B.; Li, F.; Huang, Z.; Lu, T.; Yuan, Y.; Yuan, G. Integrated catalytic process to directly convert furfural to levulinate ester with high selectivity. *ChemSusChem* **2014**, *7*, 202–209. [[CrossRef](#)] [[PubMed](#)]
17. Alamo, J.; Roy, R. Zirconium phospho-sulphates with NaZr₂(PO₄)₃-type structure. *J. Solid State Chem.* **1984**, *51*, 270–273. [[CrossRef](#)]

18. Piffard, Y.; Verbaere, A.; Kinoshita, M. β -Zr₂(PO₄)₂SO₄: A zirconium phosphato-sulphate with a Sc₂(WO₄)₃ structure. A comparison between garnet, nasicon, and Sc₂(WO₄)₃ structure types. *J. Solid State Chem.* **1987**, *71*, 121–130.
19. Thoma, S.G.; Jackson, N.B.; Nenoff, T.M.; Maxwell, R.S. Mixed Metal Phospho-Sulphates for Acid Catalysis. *Mater. Res. Soc. Symp. Proc.* **1997**, *497*, 191–199. [[CrossRef](#)]
20. Pica, M. Zirconium Phosphate Catalysts in the XXI Century: State of the Art from 2010 to Date. *Catalysts* **2017**, *7*, 190. [[CrossRef](#)]
21. Bear, I.J.; Mumme, W.G. The crystal chemistry of zirconium sulphates. VI. The structure of α -Zr(SO₄)₂. *Acta Cryst. B* **1970**, *26*, 1140–1145.
22. Ziyad, M.; Rouimi, M.; Portefaix, J.-L. Activity in hydrotreatment processes of Ni–Mo loaded zirconium phosphate Zr₃(PO₄)₄. *Appl. Catal. A* **1999**, *183*, 93–105. [[CrossRef](#)]
23. Jimenez-Morales, I.; Santamaria-Gonzales, J.; Maireles, P.; Torres, A.; Jimenez-Lopez, A. Calcined zirconium sulfate supported on MCM-41 silica as acid catalyst for ethanolysis of sunflower oil. *Appl. Catal. B: Environ.* **2011**, *103*, 91–98.
24. Escalona Platero, E.; Peñarroya Mentrut, M.; Otero Areán, C.; Zecchina, A. FTIR Studies on the Acidity of Sulfated Zirconia Prepared by Thermolysis of Zirconium Sulfate. *J. Catal.* **1996**, *162*, 268–276. [[CrossRef](#)]
25. Rack Sohn, J.; Hee Seo, D. Preparation of new solid superacid catalyst, zirconium sulfate supported on γ -alumina and activity for acid catalysis. *Catal. Today* **2003**, *87*, 219–226. [[CrossRef](#)]
26. Takarroumta, N.; Kacimi, M.; Bozon-Verduraz, F.; Liotta, L.F.; Ziyad, M. Characterization and performance of the bifunctional platinum-loaded calcium-hydroxyapatite in the one-step synthesis of methyl isobutyl ketone. *J. Mol. Catal. A* **2013**, *377*, 42–50. [[CrossRef](#)]
27. Ardizzone, S.; Bianchi, C.L. XPS characterization of sulphated zirconia catalysts: The role of iron. *Surf. Interface Anal.* **2000**, *30*, 77–80. [[CrossRef](#)]
28. Gondal, M.A.; Fasasi, T.A.; Baig, U.; Mekki, A. Effects of Oxidizing Media on the Composition, Morphology and Optical Properties of Colloidal Zirconium Oxide Nanoparticles Synthesized via Pulsed Laser Ablation in Liquid Technique. *Nanosci. Nanotechnol.* **2017**, *17*, 1–10. [[CrossRef](#)] [[PubMed](#)]
29. Yang, L.M.; Wang, Y.J.; Luo, G.S.; Dai, Y.Y. Functionalization of SBA-15 mesoporous silica with thiol or sulfonic acid groups under the crystallization conditions. *Micropor. Mesopor. Mater.* **2005**, *84*, 275–282. [[CrossRef](#)]



© 2019 by the authors. Licensee MDPI, Basel, Switzerland. This article is an open access article distributed under the terms and conditions of the Creative Commons Attribution (CC BY) license (<http://creativecommons.org/licenses/by/4.0/>).